Polymer 50 (2009) 5744–5748

Contents lists available at ScienceDirect

Polymer

journal homepage: www.elsevier.com/locate/polymer

Polymer/clay nanocomposites as VOC barrier materials and coatings

Jose M. Herrera-Alonso [a], Eva Marand [a,*], John Little [b], Steven S. Cox [b]

[a] Chemical Engineering Department, Virginia Polytechnic Institute and State University Blacksburg, VA 24061-0246, USA
[b] Department of Civil and Environmental Engineering, Virginia Polytechnic Institute and State University Blacksburg, VA 24061-0246, USA

ARTICLE INFO

Article history:
Received 30 June 2009
Received in revised form
14 September 2009
Accepted 18 September 2009
Available online 24 September 2009

Keywords:
Diffusion barrier
Clay
Nanoparticles

ABSTRACT

The transport properties of select volatile organic compounds were measured in polyurethane/clay nanocomposite barrier membranes as a function of clay content. The nanocomposites were fabricated by two different processing methods involving stirring and sonication of the clay particles. The concentration of Cloisite® 30B in the nanocomposite was varied from 0 to 50 wt%. Characterization of membrane transport properties was achieved via a gravimetric sorption method. Material-phase diffusivity coefficients (D) decreased with increasing Cloisite® concentration, while changes in the material/VOC partition coefficients (K) depended on the molecular interactions of the VOCs with the membrane material.

1. Introduction

New building materials such as structural insulating panels or SIPS have helped revolutionize the construction industry, providing improved durability, quality, high energy efficiency and affordability of housing. SIPS also make good environmental sense limiting job site waste, reducing landfill use and helping to preserve old-growth forests by using fast-growth farmed trees [1]. However SIP's ratio of cost/advantages may present certain drawbacks in other areas. Due to the manufacturing process, two outer layers and the inner core of the SIP's may contain volatile organic compounds, VOCs, such as pentene, toluene, formaldehyde, hexanal and styrene [1,2]. New houses utilizing SIPs have odor thresholds for hexanal and other aldehydes that often exceed safe limits and may remain elevated for months after construction [2,3]. The presence of VOCs in indoor air and the combined effect of tight envelope buildings prevents proper ventilation, thus, leading to degradation of indoor air quality [4]. Polymer/clay nanocomposites have been known to improve gas barrier properties [5–8], mechanical [9,10] and thermal properties [11], biodegradability [12,13], and to enhance flame retardancy [14,15]. The addition of clay nanocomposites to pristine polymers has helped improve physical properties of polymers, as was seen by the Toyota group [16–18]. We propose that the addition of clay particles to SIPs, particularly near the surface, can help reduce VOC emissions. In order to enhance these overall properties and generate improved gas barriers, dispersion and/or exfoliation of the individual silicate platelets must be achieved within the polymer matrix. Proper selection of the polymer/clay matrix is also necessary to improve the synergy between the species. The objective of this study is to develop and test nanocomposite barrier materials that substantially reduce volatile emissions to indoor air. This was achieved by evaluating the transport properties of polyurethane/clay nanocomposite membranes as a function of clay content.

2. Materials

Decane, toluene and butanol were purchased from Sigma Aldrich and were used as received. The thermoplastic polyurethane used in this study was polyether-based TPU Estane® 58315 supplied by Estane®, unit of Noveon Inc. The commercially available nanoclays were purchased from Southern Clay Products. Cloisite® 30B was used as the nanoclay for this study. This nanoclay was modified via ion-exchange with a quaternary ammomium salt that contains two hydroxyethyl groups, a methyl group and tallow group. According to the manufacturer the average concentration of the tallow (T) is as follows: ~65% C18; ~30% C16: ~5% C14, where the number following C refers to the number of carbon atoms in the tallow group. The fabrication procedure of the barrier membranes as well as the characterization of their morphology can be found in a previous publication [19]. High resolution dynamic microbalance, 0.1–0.5 μg, model D200-02 Cahn equipped with a PC-based data acquisition system was used to measure and record changes in polyurethane/clay nanocomposite sample weight during sorption/desorption cycles. Temperature within the microbalance enclosure

* Corresponding author. Tel.: +1 540 231 8231; fax: +1 540 231 5022.
E-mail address: emarand@vt.edu (E. Marand).

0032-3861/$ – see front matter © 2009 Elsevier Ltd. All rights reserved.
doi:10.1016/j.polymer.2009.09.054

was maintained at 25.7 ± 0.3 °C using a Fisher Scientific Isotemp model 1038D temperature circulator connected to a heat exchanger in the enclosure. Temperature within the sample chamber was monitored with an Omega RTD model 2Pt100G3050, temperature transducer. For sorption testing, VOC's were supplied to the microbalance at constant temperature with a diffusion cell VICI Metrometrics, Inc, Dynacalibrator Model 190. Air flow rate was controlled with mass flow controllers Tylan-General MFC model FC-280S. Rectangular shaped barrier membranes of 3.81 cm × 2.54 cm were initially dried in a vacuum oven at 100 °C for 24 h before being used in the microbalance. Calculation procedures of diffusivity coefficient, and partition coefficient can be found elsewhere [20].

3. Results and discussion

3.1. Diffusivity coefficient

The method for calculating diffusion coefficient D, of a liquid in a membrane was based on Fickian diffusion in a slab [21]. Figs. 1 and 2 depict the experimental data as well as the predicted model profile obtained from Crank's [21] time-dependent equation.

$$\frac{M_t}{M_\infty} = 1 - \frac{8}{\pi^2}\sum_{n=0}^{n=\infty}\frac{1}{(2n-1)}\exp\left\{\frac{-D(2n-1)^2\pi^2 t}{l^2}\right\} \quad (1)$$

The profile seen in Fig. 1 shows the sorption–desorption cycle for a barrier membrane containing 50 wt%. of Cloisite® 30B. Fig. 2 shows the approximation of Crank's equation to the experimental data and suggests that increasing the clay content within the polymer matrix increases the sorption equilibrium time. Due to the symmetry of the profiles the data indicates that the sorption–desorption process for all the VOC's is reversible and that D is independent of concentration. The diffusivity, D, for the VOC's in the nanocomposites as a function of clay content and processing conditions are summarized in Table 1. *N*-decane demonstrates the lowest diffusivity coefficient at all clay concentrations analyzed, while toluene has the highest value of *D*. This is consistent with the work of Ghosal and Freeman et al. [22], who demonstrate that the diffusion coefficients tend to increase with decreasing size of the penetrant VOC molecule. Table 1 also shows that increasing the nanoclay content within the polymer matrix leads to a decrease in the diffusivity for all the VOC's. Barrier membranes containing up to 50 wt% of nanoclay show a decrease in diffusivity coefficient of 87% for toluene, and butanol compared to the neat polymer. The nature of this progressive decrease can be seen in Fig. 3 in the case of toluene. The decline in the diffusivity is also relatively high for decane, which had a maximum decrease of 70% at 50 wt% concentration of Cloisite® 30B in the polyurethane compared to the neat polymer. The overall decrease in the diffusivity coefficient for the VOCs in nanocomposite films with increasing clay content may be attributed to enhanced tortuosity of the diffusion path in the matrix [23–25]. There also may be the possibility of enhanced restricted segmental motion of the polymer chains within the clay gallery space and at the interface with the clay layers [26,27] leading to lower diffusion coefficients.

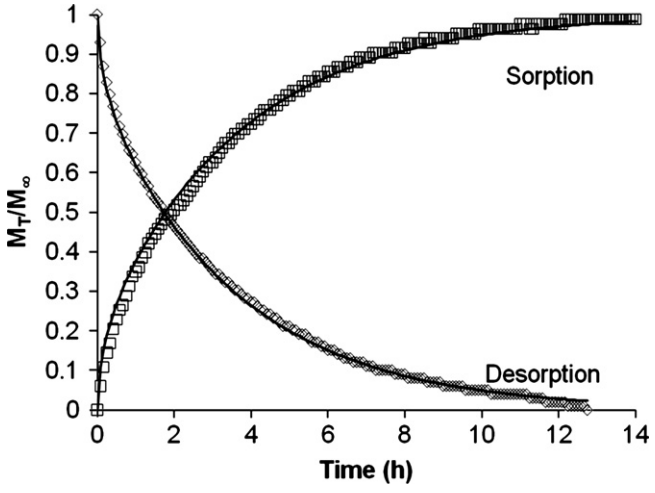

Fig. 1. Fitting of toluene transient sorption/desorption data to diffusion model of sonicated 50% wt Cloisite 30B. (◇) Desorption, (□) Sorption data, – Model.

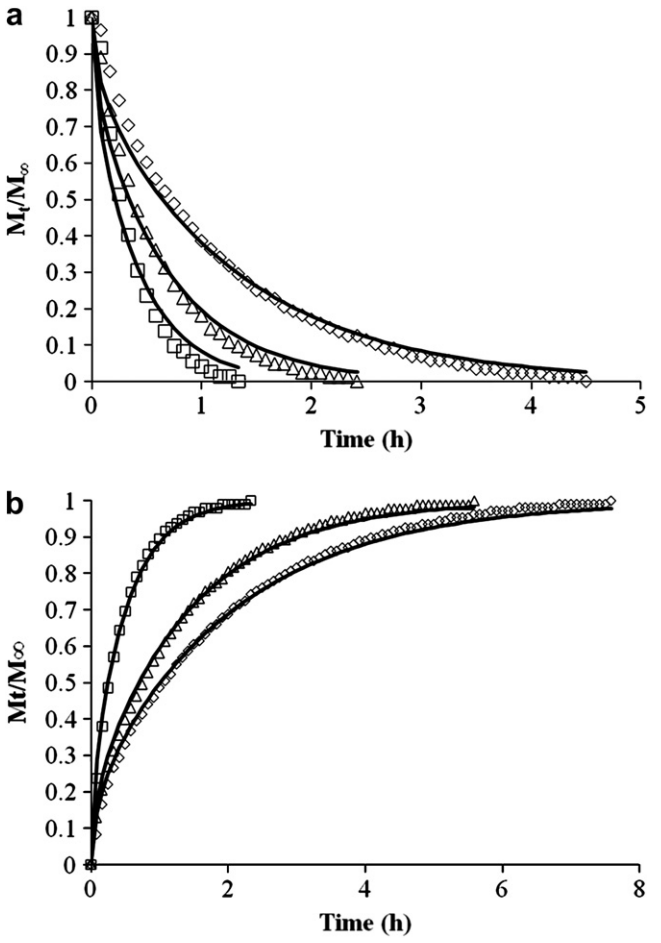

Fig. 2. Transient mass loss of (□) 17% wt Cloisite 30B, (Δ) 29% wt Cloisite 30B, (◇) 38% wt Cloisite 30B, – Model, of polyurethane/clay nanocomposite during desorption of toluene.2(b). Transient mass gain of (□) 17% wt Cloisite 30B, (Δ) 29% wt Cloisite 30B, (◇) 38% wt Cloisite 30B, – Model, of polyurethane/clay nanocomposite during sorption of *n*-butanol.

Table 1
Values of diffusivity coefficient (*D*) for different wt% of Cloisite® 30B series sorption.

Diffusivity coefficient (m^2/s)						
wt% Clay	Toluene		Decane		Butanol	
	Stirred	Sonicated	Stirred	Sonicated	Stirred	Sonicated
0	7.2 E-13	7.2 E-13	4.7 E-13	4.7 E-13	5.2 E-13	5.2 E-13
10	6.1 E-13	5.6 E-13	4.4 E-13	4.3 E-13	4.9 E-13	3.8 E-13
17	4.9 E-13	4.6 E-13	4.2 E-13	3.2 E-13	3.2 E-13	2.1 E-13
29	3.7 E-13	3.6 E-13	3.1 E-13	2.4 E-13	2.4 E-13	1.1 E-13
38	3.5 E-13	2.5 E-13	2.5 E-13	2.0 E-13	2.0 E-13	9.7 E-14
50	1.9 E-13	9.2 E-14	1.4 E-13	1.5 E-13	1.1 E-13	6.3 E-14

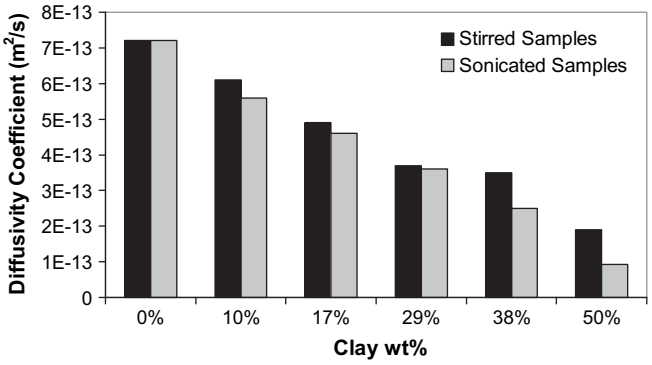

Fig. 3. Comparison of Toluene diffusivity coefficient in nanocomposites, Sonication vs Stirring Cloisite® 30B.

The processing effect of sonication is also demonstrated in Fig. 3 and also in Table 1. The data suggests that sonication of the clays during fabrication of the composites leads to a greater decrease in diffusivity coefficient when compared to samples only treated with stirring. This result reflects a higher dispersion of clay layers achieved by sonication as was shown in a previous transmission electron microscopy study [19]. The dispersion effect would further support the claim that the use of nanoclays in the polymer matrix generates more tortuous pathways for the penetrating VOC molecules [23–25].

3.2. Partition coefficient

The sorption equilibrium between the gas and solid phases, described by the partition coefficient, *K*, was obtained for toluene, decane and butanol as a function of clay content in the nanocomposites. This data is shown in Table 2. Toluene has the lowest *K* value in the series, while butanol has the highest. The partition coefficient for toluene decreases with increasing clay content, with the highest concentration of clay at 50 wt% decreasing the partition coefficient by 20% compared to the pristine polymer film. By contrast, the partition coefficient of decane increases with clay content, while that of butanol does not show any clear trends. Furthermore, the effect of processing, i.e. sonication vs. stirring does not influence the partition coefficient to a significant degree. These results can be attributed to differences in molecular interactions between the VOCs and the polymer matrix [28]. Chemical and surface modifications were made to the clay in order to improve the synergy of the natural montmorillonite with different polymers. The Na^+ group attached to the natural montmorillonite was substituted via ion exchange with an alkyl ammonium group, which renders a more hydrophobic surface and improves compatibility with the polyether based polyurethane. For example, the inverse relationship between the wt% of the clay in the matrix and the sorption values for toluene suggests that there is a repulsive interaction of toluene with the clay surface. As documented in Table 3, toluene is slightly polar, while the modified nanoclay surface is non-polar, thus prompting a decrease in *K* with increasing clay content. The opposite trend is seen with *n*-decane, whose *K* values increase with increasing clay concentration in the matrix. This suggests that there is an affinity between non-polar *n*-decane and the hydrogenated tallow tail of the alkyl ammonium group present on the nanoclay surface. As documented in Table 3, 1-butanol is highly polar and hence one would expect repulsive interactions between 1-butanol and the non-polar alkyl ammonium group. However, the data can more likely be explained by competing repulsive and attractive interactions, the latter arising from the interaction of the non-polar butane component with the alkyl group on the clay surface. In summary, the value of the partition coefficient is dominated by thermodynamic interactions and not by the morphology of the nanocomposite. This also helps explain why pre-fabrication conditions, such as sonication, do not affect the value of *K*.

Table 2
Values of partition coefficient (*K*) for different wt% of Cloisite® 30B series sorption.

Partition coefficient (*K*)						
wt% Clay	Toluene		Decane		Butanol	
	Stirred	Sonicated	Stirred	Sonicated	Stirred	Sonicated
0	1808	1808	3871	3871	4358	4358
10	1781	1712	4331	4727	4450	4022
17	1748	1687	4747	4271	4180	4106
29	1571	1602	4570	4314	4607	4160
38	1493	1550	4901	4014	4309	4218
50	1268	1460	4832	5137	3921	4127

3.3. Nanocomposites/solvent interaction parameter

To better understand the polymer-VOC interaction, we have used the sorption data to calculate the Flory–Huggins interaction parameter, χ, of the system [28,29]. This parameter estimates the interaction energy between the penetrant VOC species and the polymer segments [30]. The interaction parameter can be calculated from Eq. (2):

$$\ln a = \ln\phi + (1-\phi) + x(1-\phi)^2 \tag{2}$$

Where *a* is the activity of the penetrant vapor phase, ϕ the penetrant volume fraction and χ the polymer-penetrant interaction parameter. The activity coefficient for all the VOCs was determined from the experimental conditions by the ratio of the VOC partial pressure and the saturation vapor pressure. For the purpose of this study the specific activity of the organic vapor was maintained constant at $P = 1$ atm. The volume fraction of the penetrant VOC target molecule was determined with Eq. (3):

$$\phi = \frac{C\left(\frac{V_1}{22{,}414}\right)}{1 + C\left(\frac{V_1}{22{,}414}\right)} \tag{3}$$

where *V* is the molar volume of the penetrant VOC and C is the measured concentration of the penetrant in the polymer (ratio of cm^3 of penetrant sorbed per cm^3 of polymer) at $P = 1$ atm. As can be seen in Fig. 4., with increasing clay concentration the interaction parameter of *n*-decane decreases, from 2.5 for the pristine polyurethane to 2.27 in samples having the highest clay concentration of 50 wt%. Table 4 summarizes the χ interaction parameters for toluene, *n*-decane and 1-butanol as a function of the wt% clay in the nancomposite. In the case of toluene, the interaction parameter, χ, is negative, suggesting high solubility in the neat polymer matrix. However, the miscibility of toluene in the system decreases with the addition of clay particles modified with a hydrophobic surfactant. The opposite trend is seen with *n*-decane, whose interaction parameter decreases with wt% clay, reflecting more favorable

Table 3
Solubility parameters of the VOCs used in this study. The units of δ are $(MPa)^{1/2}$ [29]. The molar volume is expressed in cm^3/mol, and density g/ml.

VOC	δ_d Dispersion	δ_p Polarity	δ_h Hydrogen bonding	δ_s Solvent	Molar volume	Density
Toluene	18.0	1.4	2.0	18.1	106.8	0.86
1-Butanol	16.0	5.7	15.8	15.7	91.5	0.81
n-Decane	15.7	0	0	23.2	195.9	0.73

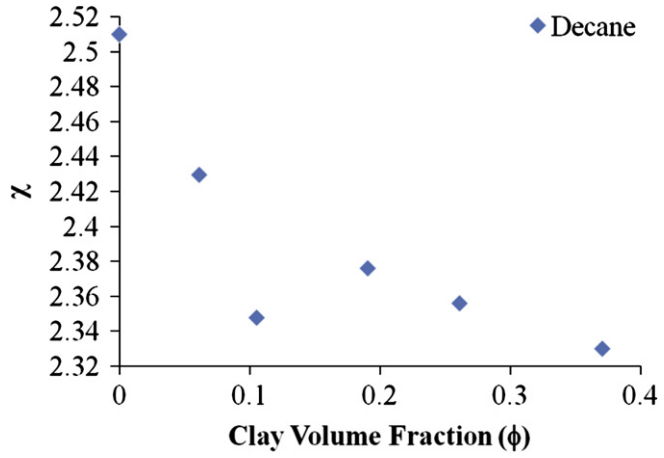

Fig. 4. Polymer/clay-VOC interaction parameter at different clay volume fraction for decane at 25 °C.

molecular interactions. Finally, the χ for 1-butanol does not follow a distinct trend. These experimental results can be compared with theoretical χ values calculated from Eq. (4) [28,29].

$$\chi = \beta + \frac{V_1(\delta_1 - \delta_2)^2}{RT} \tag{4}$$

where β is a constant equal to 0.34, V_1 is the molar volume of the penetrant, δ_1 and δ_2 are the solubility parameters of the penetrant and the polymer respectively. In order to calculate the χ interaction parameter of the membranes, the solubility coefficient δ for the polyurethane Estane® 58315 must first be determined. Different research groups evaluated this parameter via swelling measurements [31–34]. Within these groups Kim et al. [31], determined the solubility coefficient δ for a polyether based polyurethane network based on Gee's theory [35]. This theory states that in order to attain a good solubility of the polymer in the solvent, the square of the difference between the solubility parameters of the polymer and the solvent must be kept to a minimum. Gee's theory is represented by Eq. (5).

$$\frac{Q}{Q_{max}} = \exp^{\left[-\alpha Q(\delta_1-\delta_2)^2\right]} \tag{5}$$

where Q is the swelling ratio, Q_{max} is the maximum swelling ratio, α is a constant and δ_1 and δ_2 are the solubility parameters of the solvent and the polymer. The swelling ratio Q, of the polyurethane/clay nanocomposite membranes was determined by utilizing Eq. (6).

$$Q = 1 + \left(\frac{w_2}{w_1} - 1\right)\left(\frac{\rho_2}{\rho_1}\right) \tag{6}$$

where w_2 is the weight of the network at equilibrium, w_1 is the weight of the network before swelling, ρ_2 and ρ_1 are the density of the network and the density of the solvent respectively [36]. In this case the density of the polyurethane is $\rho_p = 1.12$ g/cm^3, the density of Cloisite® 30B is $\rho_c = 1.98$ and the density of the solvents are listed in Table 3. After the swelling ratio, Q, was determined for each VOC, the Q values were plotted versus the solubility parameter δ of the corresponding VOCs. The maximum swelling Q_{max}, observed for this series was seen with *n*-butanol. Once Q_{max} of the system was established and the swelling ratio Q for each VOC was also established, the solubility parameter of the polyurethane Estane® 58315 can be determined. Gee's Eq. (4) can be rearranged as follows:

$$\left[\frac{1}{Q}\ln\left(\frac{Q_{max}}{Q}\right)\right]^{0.5} = \left|\alpha^{0.5}\left(\delta_1 - \delta_2\right)\right| \tag{7}$$

The unknown parameters of the system α and δ_2, were determined by plotting the $[(1/Q)\ln(Q_{max}/Q)]^{0.5}$ vs the solubility parameters δ of the VOCs. The linearization of the data via the plotting scheme yields the parameter, $\alpha^{0.5}$, and the solubility parameter of the polyurethane, δ_2, as the slope and the intercept in the horizontal axis, respectively. The value for the calculated solubility parameter of the pure Estane® 58315 was 23.6 $(MPA)^{1/2}$, which is consistent with typical values reported for polyurethanes [37,38].

Previous studies of the nanoclays determined that the silica-alumina structure has a hydrophilic nature and the addition of the alkyl ammine group via ion exchange provides a hydrophobic property to the clay. In order determine the solubility parameter of the modified clay surface, Jang et al. [39], modeled the entire clay structure based on the longest chain of the surfactant. According to the manufacturer, Southern Clay Products, Cloisite 30Bs longest group is a hydrogenated tallow group. Thus it can be simplified by considering a linear aliphatic chain. This aliphatic chain adds a third component to the polymer-sorbent system. This additional term yields a modification in the corresponding solubility parameter of the polymer, δ_2 term of Eq. 3. This new solubility parameter is modeled via Eq. (8), as follows:

$$\bar{\delta} = \sum_i \phi_i\delta_i = \phi_1\delta_1 + \phi_2\delta_2 \tag{8}$$

Where ϕ_1 and ϕ_2, are the volume fraction of the nanoclay and of the polymer in the composite membrane, respectively. The use of Eq. (8), results in the modification of equation Eq. (4) as follows:

$$\chi = \beta + \frac{V_1\left(\delta_1 - \bar{\delta}\right)^2}{RT} \tag{9}$$

The results for the calculated χ interaction parameter of the sonicated polyurethane/clay nanocomposite membranes can be seen in Table 5. These values are similar and within the observed range found in the literature [40]. These calculated results suggest that the presence of nanoclay in the matrix leads to an increase in the miscibility of the polymer/clay composite when exposed to *n*-decane and toluene and a decrease in miscibility when exposed to 1-butanol. The decrease of the interaction parameter χ suggests that the surfactant aliphatic chain has a similar solubility parameter as *n*-decane. This is consistent with the χ interaction parameters

Table 4
Experimental interaction parameter χ, for sonicated polyurethane/clay nancomposite sonicated series.

wt% Clay	$\chi_{n\text{-decane}}$	$\chi_{toluene}$	$\chi_{1\text{-butanol}}$
0	2.51	−0.59	0.032
10	2.36	−0.54	0.112
17	2.46	−0.52	0.092
29	2.45	−0.48	0.079
38	2.52	−0.44	0.065
50	2.28	−0.38	0.087

Table 5
Calculated χ interaction parameters for pristine polyurethane Estane® 58315, and the subsequent polyurethane/clay nancomposite sonicated series.

Wt% Clay	χ *n*-decane	χ toluene	χ 1-butanol
0	3.06	1.45	0.36
10	2.78	1.28	0.34
17	2.58	1.17	0.35
29	2.22	0.97	0.40
38	1.95	0.83	0.49
50	1.56	0.64	0.71

obtained by experimental means shown in Table 4. However, experimental χ interaction parameters for toluene and 1-butanol do not follow the calculated trends. Clearly, using a mean-field model, such as Eq. (4), may be too simplistic in modeling the χ interaction parameter of polar molecules, such as 1-butanol or toluene, which have specific (directional) interactions.

4. Conclusions

Polyurethane/clay nanocomposites used as barrier membranes provide a noticeable decrease in VOC diffusivity. However, when compared to the neat polymer this decrease becomes important only at high clay content in the nano-composite. Processing methods of the barrier membranes do, in fact, influence the diffusivity, rendering better barrier properties when the clays are dispersed with sonication. Material/VOC partition coefficients, depend on the molecular interactions of the VOC with the membrane material. Thus, χ for non-polar VOC such as *n*-decane decreased with increasing clay concentration of organically modified clay in the matrix, due to favorable thermodynamic interactions. On the other hand, although the interaction parameter for toluene in the nano-composite is negative, suggesting high solubility in the polymer matrix, the addition of clay particles modified with hydrophobic alkyl groups increased the value of χ with wt% clay.

References

[1] Morley M. Building with structural insulated panels (SIPs) strength and energy efficiency through structural panel construction. Newtown, CT: Taunton Press; 2000.
[2] Hodgson AT, Beal D, McIlvaine JER. Indoor Air 2000;12(4):235–42.
[3] Hodgson AT, Rudd AF, Beal D, Chandra S. Indoor Air 2000;10(3):178–92.
[4] Liddament MW. Indoor Air 2000;10(3):193–9.
[5] Jeong HK, Krych W, Ramanan H, Nair S, Marand E, Tsapatsis M. Chemistry of Materials 2004;16(20):3838–45.
[6] Xu B, Zheng Q, Song Y, Shangguan Y. Polymer 2006;47(8):2904–10.
[7] Zhong Y, Janes D, Zheng Y, Hetzer M, De Kee D. Polymer Engineering & Science 2007;47(7):1101–7.
[8] Gain O, Espuche E, Pollet E, Alexandre M, Dubois P. Journal of Polymer Science Part B: Polymer Physics 2004;43(2):205–14.
[9] Chavarria F, Paul DR. Polymer 2006;47(22):7760–73.
[10] Wang Z, Pinnavaia TJ. Chemistry of Materials 1998;10(12):3769–71.
[11] Yoon PJ, Fornes TD, Paul DR. Polymer 2002;43(25):6727–41.
[12] Ray SS, Okamoto K, Okamoto M. Macromolecules 2003;36(7):2355–67.
[13] Ray SS, Yamada K, Okamoto M, Ueda K. Nano Letters 2002;2(10):1093–6.
[14] Beyer G. Plastics, Additives and Compounding 2002;4(10):22–8.
[15] Zheng X, Wilkie CA. Polymer Degradation and Stability 2003;81(3):539–50.
[16] Kojima Y, Fukumori K, Usuki A, Okada A, Kurauchi T. Journal of Materials Science Letters 1993;12(12):889–90.
[17] Kojima Y, Usuki A, Kawasumi M, Okada A, Kurauchi T, Kamigaito O. Journal of Applied Polymer Science 1993;49(7):1259–64.
[18] Usuki A, Kojima Y, Kawasumi M, Okada A, Fukushima Y, Kurauchi T, et al. Journal of Materials Research 1993;8(5):1179–84.
[19] Herrera-Alonso JM, Marand E, Little JC, Cox SS. Journal of Membrane Science 2009;337(1-2):208–14.
[20] Cox SS, Zhao D, Little JC. Atmospheric Environment 2001;35(22):3823–30.
[21] Crank J. The mathematics of diffusion. New York: Oxford University Press; 1979.
[22] Ghosal K, Freeman BD. Polymers for Advanced Technologies 1994;5(11):673–97.
[23] Eitzman DM, Melkote RR, Cussler EL. AIChE Journal 1996;42(1):2–9.
[24] Nielsen LE. Journal of Macromolecular Science Chemistry 1967;A1:929–42.
[25] Perry D, Ward WJ, Cussler EL. Journal of Membrane Science 1989;44(2-3):305–11.
[26] Finnigan B, Halley P, Jack K, McDowell A, Truss R, Casey P, et al. Journal of Applied Polymer Science 2006;102(1):128–39.
[27] Mondal S, Hu JL. Journal of Membrane Science 2006;274(1-2):219–26.
[28] Prausnitz JM, Lichtenthaler RN, Gomes de Azevedo E. Molecular thermodynamics of fluid-phase equilibria. 3rd ed. Upper Saddle River, New Jersey: Prentice Hall PTR; 1999.
[29] Hansen CM. Hansen solubility parameters: a user's handbook. 2nd ed. Boca Raton, FL: CRC Press; 2007.
[30] Merkel TC, Bondar VI, Nagai K, Freeman BD, Pinnau I. Journal of Polymer Science: Part B: Polymer Physics 2000;38(3):415–34.
[31] Kim CK, Bae SB, Ahn JR, Chung IJ. Polymer Bulletin 2008;61:225–33.
[32] Roşu D, Ciobanu C, Caşcaval CN. Journal of Applied Polymer Science 2001;80:1802–13.
[33] Ajithkumar S, Patel NK, Kansara SS. European Polymer Journal 2000;36:2387–93.
[34] Gopakumar S, Gopinathan Nair MR. European Polymer Journal 2005;41:2002–9.
[35] Gee G. Transactions, Institution of the Rubber Industry 1943;18:266–81.
[36] Rabek JF. Experimental methods in polymer chemistry. New York: John Wiley & Sons, Inc; 1980.
[37] Ebdon JR, Hourston DJ, Klein PG. Polymer 1984;25:1633–9.
[38] Mieczkowski R. European Polymer Journal 1992;28(1):53–5.
[39] Jang BN, Wang D, Wilkie CA. Macromolecules 2005;38(15):6533–43.
[40] Wolińska-Grabczyk A. Journal of Membrane Science 2007;302(1–2):59–69.